Journal of Medicinal Chemistry

Article

pubs.acs.org/jmc

Structure−Activity Relationship Studies toward the Discovery of Selective Apelin Receptor Agonists

Jean-François Margathe,[†,§] Xavier Iturrioz,[‡,§] Rodrigo Alvear-Perez,[‡] Claire Marsol,[†] Stéphanie Riché,[†] Hadjila Chabane,[‡] Nassera Tounsi,[†] Maxime Kuhry,[†] Denis Heissler,[†] Marcel Hibert,[†] Catherine Llorens-Cortes,*[,‡,∥] and Dominique Bonnet*[,†,∥]

[†]Laboratoire d'Innovation Thérapeutique, UMR7200 CNRS/Université de Strasbourg, Labex Medalis, Faculté de Pharmacie, 74 route du Rhin, 67401 Illkirch, France

[‡]Laboratory of Central Neuropeptides in the Regulation of Body Fluid Homeostasis and Cardiovascular Functions, Center for Interdisciplinary Research in Biology (CIRB), Collège de France, INSERM U1050, CNRS UMR7241, 75005 Paris, France

Supporting Information

ABSTRACT: Apelin is the endogenous ligand for the previously orphaned G protein-coupled receptor APJ. Apelin and its receptor are widely distributed in the brain, heart, and vasculature, and are emerging as an important regulator of body fluid homeostasis and cardiovascular functions. To further progress in the pharmacology and the physiological role of the apelin receptor, the development of small, bioavailable agonists and antagonists of the apelin receptor, is crucial. In this context, E339−3D6 (**1**) was described as the first nonpeptidic apelin receptor agonist. We show here that **1** is actually a mixture of polymethylated species, and we describe an alternative and versatile solid-phase approach that allows access to highly pure **27**, the major component of **1**. This approach was also applied to prepare a series of derivatives in order to identify the crucial structural determinants required for the ligand to maintain its affinity for the apelin receptor as well as its capacity to promote apelin receptor signaling and internalization. The study of the structure−activity relationships led to the identification of ligands **19**, **21**, and **38**, which display an increased affinity compared to that of **27**. The latter and **19** behave as full agonists with regard to cAMP production and apelin receptor internalization, whereas **21** is a biased agonist toward cAMP production. Interestingly, the three ligands display a much higher stability in mouse plasma ($T_{1/2}$ > 10 h) than the endogenous apelin-17 peptide **2** ($T_{1/2}$ < 4 min).

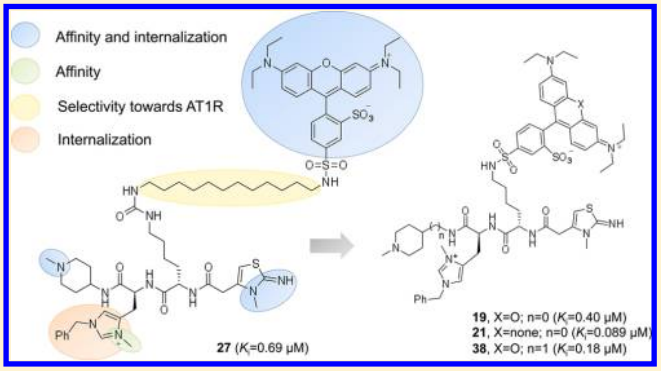

INTRODUCTION

Apelin is a neuro-vasoactive peptide, isolated from bovine stomach extracts,[1] and identified as the endogenous ligand of the human APJ orphan receptor (subsequently named ApelinR for apelin receptor) that shares 31% sequence identity with the angiotensin II receptor type 1 (AT1R).[2] The ApelinR is 380 amino acid long and was identified as a member of the seven transmembrane-domain G protein-coupled receptors (GPCR) family. It has also been cloned in mice[3] and rats.[4] Apelin derives from a single 77-amino acid precursor named preproapelin.[1,5,6] The alignment of preproapelin amino acid (aa) sequences from mammalian species demonstrates a fully conserved C-terminal 17-aa sequence **2** (Lys-Phe-Arg-Arg-Gln-Arg-Pro-Arg-Leu-Ser-His-Lys-Gly-Pro-Met-Pro-Phe called apelin-17 or K17F),[5] including apelin-13 (Gln-Arg-Pro-Arg-Leu-Ser-His-Lys-Gly-Pro-Met-Pro-Phe). The N-terminal glutamine residue of the latter peptide might be lactamized to produce the pyroglutamyl form **3** (pGlu-Arg-Pro-Arg-Leu-Ser-His-Lys-Gly-Pro-Met-Pro-Phe called pE13F).[5] Both peptides **2** and **3** are the predominant molecular forms of apelin in the rat brain and in rat and human plasma.[7,8] They exhibit a high affinity for the human and the rat apelin receptors, although **2** has a 10 times higher affinity than **3** for the human or rat ApelinR.[9−11] They similarly inhibit forskolin-induced cAMP production in cells expressing either the human[5,10] or the rat ApelinR.[4,12] Both peptides are potent inducers of ApelinR internalization in a clathrin-dependent manner with a higher potency for **2** than for **3**.[10,13−15]

Apelin and its receptor are widely distributed in the brain[4,6,16−18] where they colocalize with arginine vasopressin (AVP) in magnocellular neurons.[8,19,20] Central injection of **2** in lactating rats inhibits the electrical activity of AVP neurons, thereby decreasing AVP release into the bloodstream and increasing aqueous diuresis.[8] Moreover, AVP and apelin levels are conversely regulated by osmotic and volemic stimuli in humans and rodents to maintain body fluid homeostasis.[7,8,20]

Apelin and its receptor are also present in the cardiovascular system.[21] Several studies pointed out the role of apelin in the

Received: November 18, 2013
Published: March 13, 2014

control of cardiovascular functions: apelin increases the contractile force of the myocardium by a positive inotropic effect,[22−24] and apelin gene-deficient mice subjected to chronic pressure overload developed severe and progressive heart failure.[25] Moreover, intravenous injection of **2** or **3** in rodents decreases arterial blood pressure (BP),[6,13,15] through nitric oxide production[26] with a more marked effect for **2** than for **3**.[13] In contrast, the deletion of the C-terminal Phe in **2** or the Ala substitution of the C-terminal Phe in **3** suppressed the ability of **2** and **3** to decrease BP,[13,27] suggesting that the hypotensive activity of apelin required the presence of the C-terminal Phe residue. Since we recently showed that the C-terminal Phe residue of **2** plays a crucial role in ApelinR internalization but not in apelin binding or in $G_{\alpha i}$-protein coupling,[9] this suggests that the decrease in blood pressure induced by **2** requires ApelinR internalization and/or involves another yet to be discovered signaling pathway.

In addition, apelin has been shown to modulate the adipoinsular axis: a systemic injection of apelin in insulin-resistant mice decreases glycemia and enhances glucose uptake in skeletal muscle and adipose tissue, contributing to homeostatic control of blood glucose.[28] However, **2** displays a short half-life in the blood circulation in mice (in the minute range; personal data), and **3** is metabolized. Therefore, to facilitate the *in vivo* evaluation of apelin effects, it is of importance to discover more stable small molecular probes, agonists and antagonists of the ApelinR to further investigate the physiopathological roles played by apelin and its receptor.

To date, very few nonendogenous ligands have been described in the literature.[29,10] The synthesis of cyclic analogues of the minimal fragment apelin-12 (Arg-Pro-Arg-Leu-Ser-His-Lys-Gly-Pro-Met-Pro-Phe) was described as a strategy to potentially improve the bioactivity, selectivity, and bioavailability of apelin.[30] The Arg-Pro-Arg sequence was also explored to design and to synthesize antagonist cyclic peptides with micromolar affinity for the ApelinR.[31,32] Nevertheless, these ligands exhibit high molecular weights and low affinity and/or efficacy for the ApelinR. More recently, 4-oxo-6-(pyrimidin-2-ylthiomethyl)-4*H*-pyran-3-yl 4-nitrobenzoate (ML221), coming from the screening of the NIH small molecule collection, was identified and described as an apelin functional antagonist with regard to the inhibition of cAMP production.[33]

Prior to these disclosures, in order to accelerate the discovery of ligands for orphan GPCR, we have set up an original FRET-based assay that consists of screening fluorescent small organic compound libraries on enhanced green fluorescent protein (EGFP)-fused GPCR.[34] Applied to ApelinR, this approach enabled the successful discovery of the first nonpeptidic ApelinR agonist, E339−3D6 (**1**).[12] The latter behaves as a partial agonist with regard to cAMP production and as a full agonist with regard to ApelinR internalization. As apelin, **1** was found to induce vasorelaxation of rat aorta precontracted by noradrenaline, and when centrally injected, potently inhibited AVP release in the blood circulation in water-deprived mice.

The pharmacological interest of **1** prompted us to study further the structure−activity relationships around this compound with the aim (1) to identify the important structural determinants of the ligand required for its affinity for the ApelinR as well as for its capacity to promote ApelinR signaling and internalization; (2) to develop more potent ApelinR agonists; (3) to increase the binding selectivity toward the ApelinR versus AT1R; (4) to decrease its size and improve its metabolic stability. Herein, we report a solid-phase strategy to access a series of compound **1** derivatives, evaluated for their affinity for the ApelinR. The highest affinity compounds were assessed for their ability to inhibit cAMP production and to trigger ApelinR internalization in CHO cells stably expressing the rat ApelinR tagged at its C-terminal part with EGFP. The selectivity of these compounds toward the AT1R was also investigated together with their plasma stability.

CHEMISTRY

The synthesis of **1** was originally achieved by a solid-phase strategy based on the regenerative Michael acceptor (REM) resin.[12,35] This approach involves the release of the final product from the solid-support via a Hofmann elimination, which requires the treatment of the resin with an excess of methyl iodide (40 equiv). The RP-HPLC analysis of purified **1** showed a single peak (Supporting Information, Figure S1). We thus expected to have a compound with structure **27** (Figure 1). However, ES-MS analysis of the purified product clearly

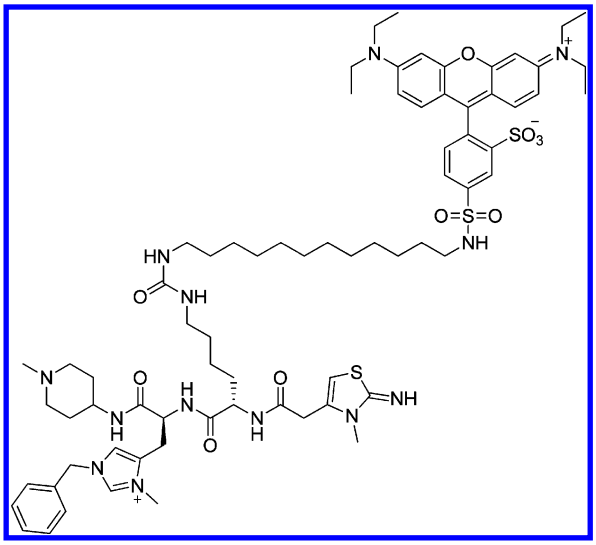

Figure 1. Chemical structure of **27**, the major component of **1**.[12]

showed the presence, in addition to **27**, of several polymethylated compounds that could not be isolated by RP-HPLC, regardless of the nature of the column and the mobile phase (Figure 2A). The presence of three major methylated forms was confirmed by analytical capillary zone electrophoresis (Supporting Information, Figure S2). MS/MS experiments performed on **1** followed by analysis of the various fragments allowed us to identify the number and the location of the different methyl groups. The analysis clearly showed that no methyl group was incorporated on Lissamine Rhodamine B (LRB), whereas there was one methyl on the iminothiazolyl, one or none on the 3-benzyl imidazolyl, and one or two on the piperidyl ring (Supporting Information, Figure S3). These results prompted us to devise an alternative and versatile solid-phase approach to access fully defined and characterized **27**, as well as a series of derivatives to study the structure−activity relationships around **27** (Scheme 1).

Starting from commercially available 2-(3,5-dimethoxy-4-formylphenoxy)ethyl (DFPE)-PS resin, *N*-Boc-4-aminopiperidine was anchored to the solid support by reductive amination in the presence of $NaBH_3CN$.[36] Then, the acylation of the resulting secondary amine with Fmoc-L-His(Bzl)-OH led to resin **9**. A selective methylation of the imidazole ring at the N-3

dx.doi.org/10.1021/jm401789v | J. Med. Chem. 2014, 57, 2908−2919

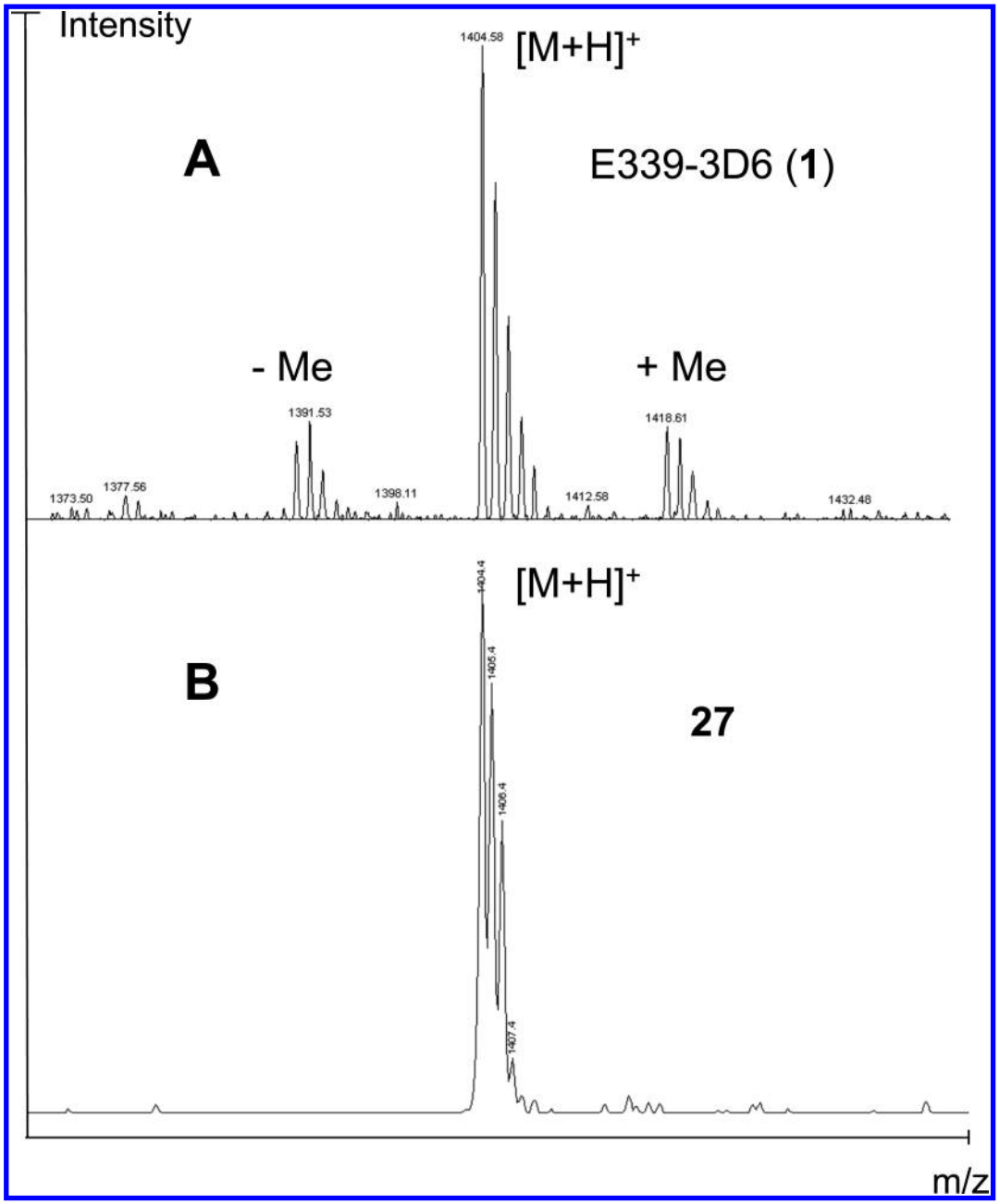

Figure 2. ES-MS profiles: (A) **1** obtained on REM resin and (B) **27** obtained on DFPE resin.

position in the presence of MeI was followed by the removal of the *N*-Boc protecting group by treatment with trimethylsilyl trifluoromethanesulfonate (TMSOTf)/lutidine.[36,37] Twice 30 min was found to be the optimal duration in order to drive the piperidine deprotection to completion while avoiding any premature cleavage of the product from the resin. Reductive alkylation of the deprotected piperidine with formaldehyde led to resin **11**. Following a classical Fmoc/*t*-butyl approach, Fmoc-L-Lys(ivDde)-OH and (2-(Boc)imino-3-methyl-2,3-dihydrothiazol-4-yl)acetic acid (**8**) were incorporated on solid support via (benzotriazol-1-yl-oxy)trispyrrolidinophosphonium hexafluorophosphate (PyBOP) activation. Then, the 1-(4,4-dimethyl-2,6-dioxocyclohex-1-ylidene)-3-methylbutyl (ivDde) protecting group was removed in the presence of 2% hydrazine in DMF providing resin **13**. The deprotected ε-amino group was then reacted with *p*-nitrophenyl chloroformate followed by the addition of an excess of 1,12-dodecanediamine to provide resin **23**. Sulfonylation of this resin with Lissamine Rhodamine B sulfonyl chloride (LRB-Cl), obtained by treatment of Acid Red 52 sodium salt with oxalyl chloride,[38] yielded resin **25**. A final treatment with TFA enabled the cleavage of compound **27** from the solid support, followed by its isolation by RP-HPLC. In contrast to **1**, ES-MS analysis of the purified **27** showed that it was obtained as a unique and well-defined trimethylated form (Figure 2B). Thanks to this convenient and flexible solid-phase approach, compounds derived from **27** were thus obtained in moderate to good yields. The purity and the identity of the compounds were checked by analytical RP-HPLC, liquid chromatography−mass spectrometry (LC-MS), and high resolution mass spectrometry (HRMS).

As depicted in Scheme 2, compound **8** was obtained in a three-step process starting from commercially available ester **4**.

dx.doi.org/10.1021/jm401789v | *J. Med. Chem.* 2014, 57, 2908−2919

Scheme 1. General Solid-Phase Strategy for the Synthesis of 27 and Derivatives[a]

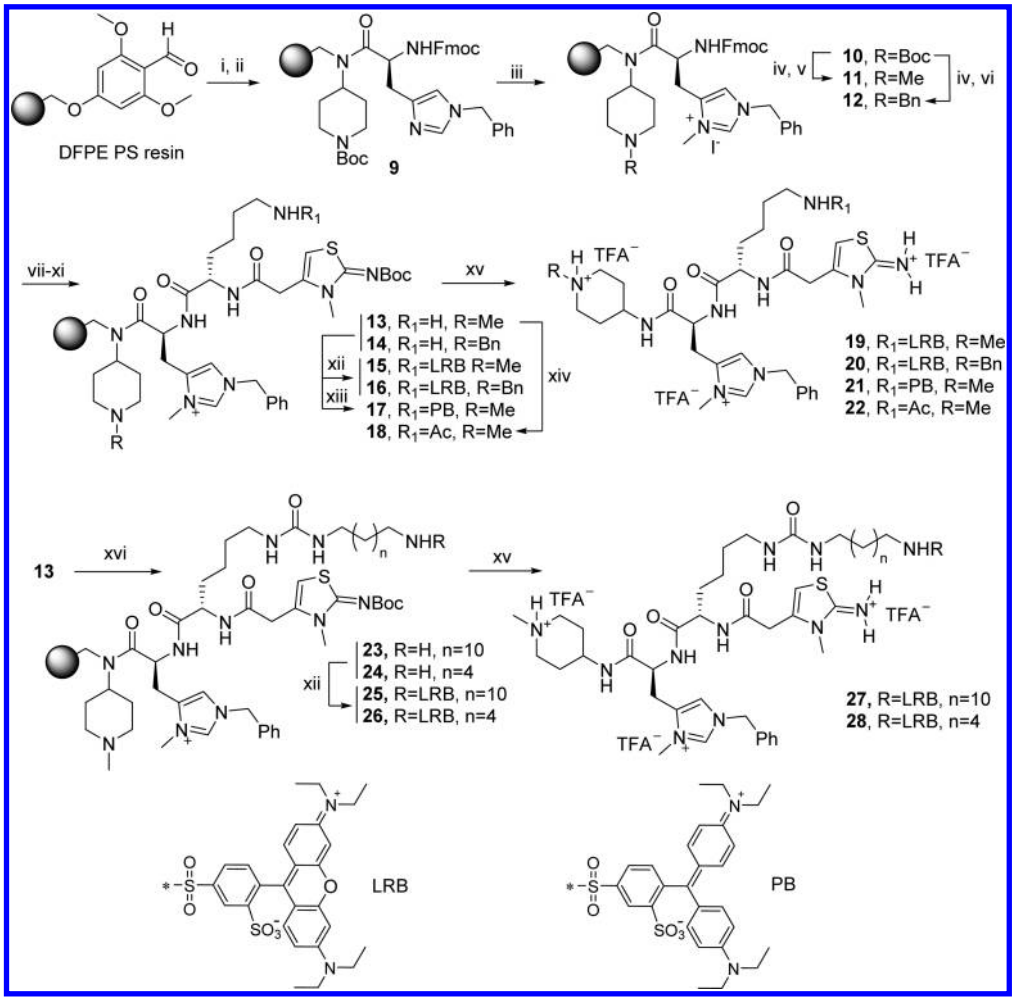

[a]Reagents: (i) 4-Amino-1-Boc-piperidine, $NaBH_3CN$, DMF/MeOH/AcOH, 60 °C, 24 h; (ii) Fmoc-His(1-Bzl)-OH, HATU, DIEA, CH_2Cl_2/DMF, rt, overnight; (iii) MeI, DMF, 40 °C, overnight; (iv) TMSOTf, 2,6-lutidine, rt, 2 × 30 min; (v) H_2CO, THF/$HC(OMe)_3$, rt, 5 h then $NaBH(OAc)_3$, 1,2-DCE, rt, overnight; (vi) PhCHO, THF/$HC(OCH_3)_3$, rt, 5 h then $NaBH(OAc)_3$, $ClCH_2$−CH_2Cl, rt, overnight; (vii) Piperidine, DMF, rt, 2 × 15 min; (viii) Fmoc-Lys(ivDde)-OH, PyBOP, HOBt, DIEA, DMF, rt, 2 h; (ix) piperidine, DMF, rt, 2 × 15 min; (x) **8**, PyBOP, HOBt, DIEA, CH_2Cl_2/DMF, rt, overnight; (xi) N_2H_4 hydrate, DMF, rt, 3 × 5 min; (xii) LRB-Cl, DIEA, CH_2Cl_2, rt, 5 h; (xiii) PB-Cl, DIEA, CH_2Cl_2, rt, 5 h; (xiv) Ac_2O, DIEA, CH_2Cl_2, rt, 2 × 10 min; (xv) TFA/H_2O/*i*-Pr_3SiH, rt, 3 h; (xvi) *p*-NO_2−C_6H_4−OCOCl, DIEA, THF/CH_2Cl_2, rt, 2 × 45 min then $H_2NCH_2(CH_2)_nCH_2NH_2$, DIEA, CH_2Cl_2, 30 °C, overnight.

Scheme 2. Synthesis of Compound 8[a]

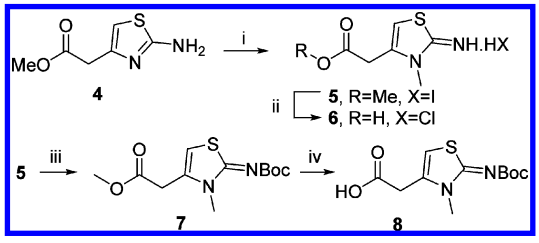

[a]Reagents: (i) MeI, THF, rt, 3 d, 96%; (ii) 1 N HCl, dioxane/H_2O, 40 °C, overnight, 88%; (iii) Boc_2O, 4-DMAP, pyridine, CH_2Cl_2, 0 °C to rt, 2 h, 44%; (iv) LiOH, dioxane/H_2O, 40 °C, 1 h, 61%.

As previously described for the synthesis of 2-imino-3-alkyl thiazoline,[39] methylation at the N-3 position was achieved by treatment with MeI at room temperature for 3 days, affording derivative **5** in excellent yield (96%). Ester hydrolysis under acidic conditions provided acid **6**. Alternatively, the imino moiety of **5** was protected with a Boc group (44%) to avoid acylation, which occurred in preliminary experiments during the solid-phase incorporation of **6**. Basic hydrolysis of the protected compound **7** led to acid **8** in 61% yield, ready for introduction on solid-phase.

RESULTS AND DISCUSSION

Following our recent discovery of **1**, the first nonpeptidic agonist for ApelinR, a structure−activity relationship study was undertaken. As **1** was shown to be actually a mixture of diversely methylated compounds, our first objective was to identify the contribution of five of them to the activity of the mixture. Thanks to the novel solid-phase approach developed on DFPE-PS resin, compounds **27** and **29**−**32** were produced by changing the number and the position of the methyl groups. Their affinities for the ApelinR were then evaluated by a radioligand binding assay (Table 1).

Binding Affinities of the Various Methylated Components of 1. Interestingly, with the exception of **32**, the affinity remains in the micromolar range indicating that the methylation pattern is not the key component of the affinity

dx.doi.org/10.1021/jm401789v | J. Med. Chem. 2014, 57, 2908−2919

Table 1. Inhibition Constants of Methylated Components of 1

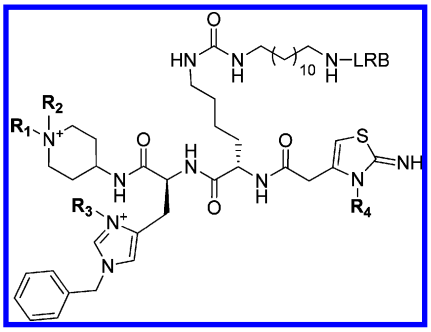

cpd	R_1	R_2	R_3	R_4	K_i (μM)[a,b]
27	-Me	-H	-Me	-Me	0.69 ± 0.12
29	-Me	-Me	-Me	-Me	1.4 ± 0.1
30	-Me	-Me		-Me	3.0 ± 1.0
31	-Me	-H		-Me	1.5 ± 0.3
32	-Me	-H		-H	9.0 ± 4.0

[a]The inhibition constants (K_i) of compounds for the ApelinR were determined on CHO cell membranes stably expressing the human ApelinR by a competition binding assay using as radioligand [^{125}I]-**3**. Data represent the means ± SEM of 3 to 10 independent experiments performed in duplicate. [b]K_i value for **1** is 0.43 ± 0.04 μM.

of **1** (Table 1). However, some significant trends can be observed. For instance, the best affinity for ApelinR was found for the trimethylated derivative **27** (K_i = 0.69 μM). The tetramethylated compound **29** bearing two methyl groups on the piperidyl ring displayed a 2-fold decrease in affinity (K_i = 1.4 μM). In the absence of a methyl group on the 3-benzyl-imidazolyl ring, similar affinities were obtained for the dimethylated compound **31** (K_i = 1.5 μM) and the trimethylated species **30** (K_i = 3.0 μM). These results tend to demonstrate the importance of the imidazolium ring to retain a submicromolar affinity for the ApelinR. Finally, the suppression of the methyl group on the thiazoline ring in **32** led also to an important decrease in affinity (K_i = 9.0 μM). This result may be ascribed to the influence of the methylation at the N-3 position of the aminothiazolyl ring on the basicity of the exocyclic nitrogen group. Indeed, as determined by potentiometry in a water medium, the pK_a values of **4** and **5** were found to be 4.83 ± 0.02 and 9.77 ± 0.02, respectively. Consequently, at physiological pH, the imino moiety is mainly protonated when the endocyclic nitrogen is methylated. This result suggests that the more basic imino form combined with the presence of the methyl group favors the binding of the ligand to the ApelinR.

Influence of the Length of the Spacer. Having determined the most potent methylated form, compound **27**, we next examined the influence of the length of the spacer between the LRB group and the rest of the molecule on the affinity for the ApelinR. Table 2 shows that shortening the spacer from 12 to 6 carbon atoms as in **28** resulted in a 2-fold increase in affinity (from K_i = 0.69 to 0.31 μM). Surprisingly, the direct incorporation of LRB on the ε-amino group of the lysinyl core is not detrimental to the affinity. Indeed, the K_i of **19** is still 0.40 μM, even better than that determined for **27**. These data suggest that LRB does not bind ApelinR at the level of the aromatic pocket as we previously suggested[12] but more likely at the surface of the receptor or less deeply in the receptor transmembrane bundles. However, the removal of the

Table 2. Influence of the Length of the Spacer and the Presence of LRB Dye on Binding Affinities for the ApelinR

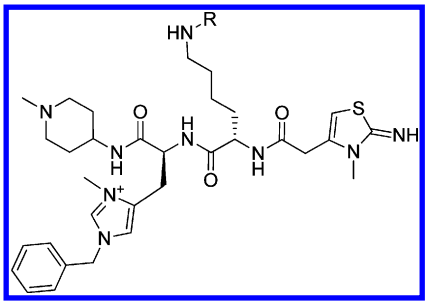

cpd	R	K_i (μM)[a]
27	-CONH$(CH_2)_{12}$NH-LRB	0.69 ± 0.12
28	-CONH$(CH_2)_6$NH-LRB	0.31 ± 0.07
19	-LRB	0.40 ± 0.08
21	-PB	0.089 ± 0.014
22	-COMe	>100
33	*n*-BuNH-LRB	>100

[a]The inhibition constants (K_i) of compounds for the ApelinR were determined on CHO cell membranes stably expressing the human ApelinR by a competition binding assay using as radioligand [^{125}I]-**3**. Data represent the means ± SEM of 3 to 10 independent experiments performed in duplicate.

LRB group resulted in a total loss of affinity (**22**), indicating the crucial role played by LRB in the binding mode of the ligand. However, as demonstrated with **33**, the LRB moiety alone was found unable to bind to the ApelinR. Interestingly, the substitution of LRB for the structurally close Patent Blue (PB) enabled us to increase the affinity of the resulting compound **21** to a value of 89 nM.

Influence of the Heterocyclic Substituents. In the next step, the influence of the 1-methyl-4-piperidyl (**X** group), 1-methyl-3-benzyl-imidazolium (**Y** group), and 2-imino-3-methyl-thiazol-4-yl (**Z** group) substituents on the binding affinity of the resulting compounds for the ApelinR was carefully investigated (Table 3). The substitution of **X** for propanamide linked at C-2

Table 3. Influence of the Nature of the Substituents X, Y, and Z on the Binding Affinities of Compounds 34−36 for the ApelinR

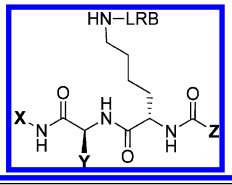

Cpd	X	Y	Z	K_i (μM)[a]
34		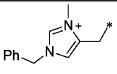	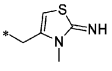	0.97 ± 0.10
35	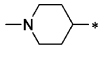	-Me	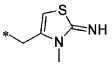	0.45 ± 0.07
36	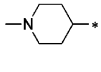	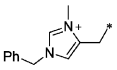	-Me	1.20 ± 0.01

[a]The inhibition constants (K_i) of compounds for the ApelinR were determined on CHO cell membranes stably expressing the human ApelinR by a competition binding assay using as radioligand [^{125}I]-**3**. Data represent the means ± SEM of 3 to 4 independent experiments performed in duplicate.

dx.doi.org/10.1021/jm401789v | J. Med. Chem. 2014, 57, 2908−2919

(**34**) or of **Z** for a methyl group (**36**) led to a decrease in the affinity for both compounds (2.5- and 3-fold, respectively), whereas the substitution of **Y** for a methyl group (**35**) did not modify the affinity for the ApelinR (K_i = 0.45 μM). The imidazolium group seems important for the affinity only when a long spacer (C_{12}) between the LRB and the trimethylated part of the compound is present (**31**). When the spacer is removed, then the benzyl substituted imidazolium can also be suppressed without loss of affinity (**35**, K_i = 0.45 μM).

Influence of the Basicity of the Heterocyclic Substituents. To further evaluate the influence of the basicity of the heterocyclic substituents on the affinity of **19** (Table 4), 1-methyl-4-piperidyl was switched to the tetrahydropyran moiety, not charged at physiological pH (**37**), leading to a 2.5-fold decrease in the affinity of the compound for the ApelinR. Interestingly, switching to 1-benzyl-4-piperidyl (**20**) or (1-methyl-4-piperidyl)methyl (**38**) groups at the **X** position resulted in a slight increase in the affinity of these compounds as compared to **27** (respectively, 0.27 and 0.18 vs 0.40 μM). Finally, the suppression of the methyl group on imidazole or iminothiazoline rings (compounds **39** and **40**, respectively) led to a 2-fold decrease in the affinity (0.96 and 0.85 μM, respectively) of these compounds as compared to **19**.

Table 4. Influence of the Basicity of the Heterocyclic Substituents on Binding Affinities for the ApelinR

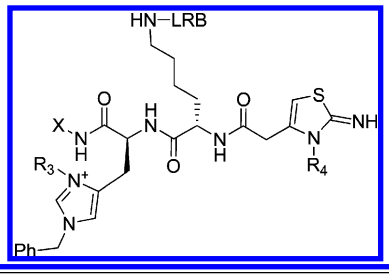

Cpd	X	R_3	R_4	K_i (μM)[a]
37		Me	Me	0.98 ± 0.10
38	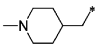	Me	Me	0.18 ± 0.08
20	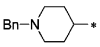	Me	Me	0.27 ± 0.03
39		-	Me	0.96 ± 0.10
40		Me	-	0.85 ± 0.03

[a]The inhibition constants (K_i) of compounds for the ApelinR were determined on CHO cell membranes stably expressing the human ApelinR by a competition binding assay using as radioligand [^{125}I]-**3**. Data represent the means ± SEM of 3 to 4 independent experiments performed in duplicate.

Ability of the Ligands to Trigger ApelinR Internalization. Confocal microscopic analysis of CHO cells stably expressing the rat ApelinR-EGFP in resting conditions displayed intense ApelinR-EGFP fluorescence at the plasma membrane (Figure 3) as described previously.[13] Incubation with **2** (100 nM) for 20 min resulted in a massive internalization of the ApelinR/**2** complexes (Figure 3A). We then tested the capacity of **27** to trigger ApelinR internalization. Incubation of CHO cells with increasing concentrations of **27** (100 μM) for 20 min resulted in ApelinR-EGFP internalization. Total internalization of the ApelinR occurred for concentrations of **27** comprised between 10 and 100 μM (Figure 3A), suggesting that **27** behaves as a full agonist with regard to ApelinR internalization.

As demonstrated with **28** and **19**, the length of the spacer has a low impact on the agonist character of ligands. Indeed, both ligands are still able to induce ApelinR internalization at the same concentration than **1** and **27** (Figure 3A). In contrast, the substitution of LRB for the structurally close PB results in the modification of the ability of the ligand to induce ApelinR internalization. Indeed, the cells treated with **21** exhibited no or very weak receptor internalization even at a high concentration (Figure 3B), showing the importance of LRB to ensure the agonist character of the ligand related to ApelinR internalization. The ability of **21** to behave as an ApelinR antagonist with regard to ApelinR internalization was then evaluated. Competition experiments were performed in the presence of **2** at 1 and 10 nM. Confocal microscopy analysis showed that **21** (100 μM) did not block or modify the ability of **2** to trigger ApelinR internalization (Figure 3B). This result indicates that **21** is not an ApelinR antagonist on ApelinR internalization.

Other structural determinants are important for the ability of the ligand to ensure ApelinR internalization. The introduction at the **X** position of 1-benzyl-4-piperidyl or (1-methyl-4-piperidyl)methyl groups (compounds **38** and **20**, respectively) did not affect the ability of the ligands to induce ApelinR internalization (Supporting Information, Figure S4). The suppression of the methyl group at N-1 of benzyl-imidazolium also had a low impact on the potency of **39**. However, the total suppression of the benzyl imidazolium group (**35**) resulted in the inability of the compound to induce ApelinR internalization. A similar result was obtained when the piperidyl moiety was switched to the neutral tetrahydropyran group. Indeed, **37** was no longer able to induce ApelinR internalization (Supporting Information, Figure S4), demonstrating the crucial role of the cationic piperidyl group on the potency of the ligand to trigger ApelinR internalization. Finally, the removal of the methyl at N-3 of iminothiazoline (**40**) was also found detrimental for ligand-induced ApelinR internalization (Supporting Information, Figure S4).

Figure 4 summarizes the important features of the structure–activity relationships around **27**. LRB, 1-methyl piperidyl, and 2-imino-3-methylthiazolyl groups play a crucial role in both the affinity and the potency of **27** to induce ApelinR internalization. The 3-benzyl imidazolyl group has only an influence on the potency of **27** to induce ApelinR internalization, whereas its *N*′ methylation has a low but significant impact on its affinity. Finally, the length of the spacer between the LRB group and the rest of the molecule has no influence on both the affinity and the potency of **27** to induce ApelinR internalization.

From the structure–activity relationship study around **27** emerged **19** and **21** that exhibited a lower molecular weight and improved binding affinities for ApelinR as compared to **27**, but with different pharmacological properties. To further characterize these three new ligands and to determine the best candidates for further *in vivo* evaluation, we decided to investigate (1) their binding selectivity toward angiotensin II receptor type 1 (AT1R), which exhibits the highest amino acid sequence identity compared to that of ApelinR in the GPCR

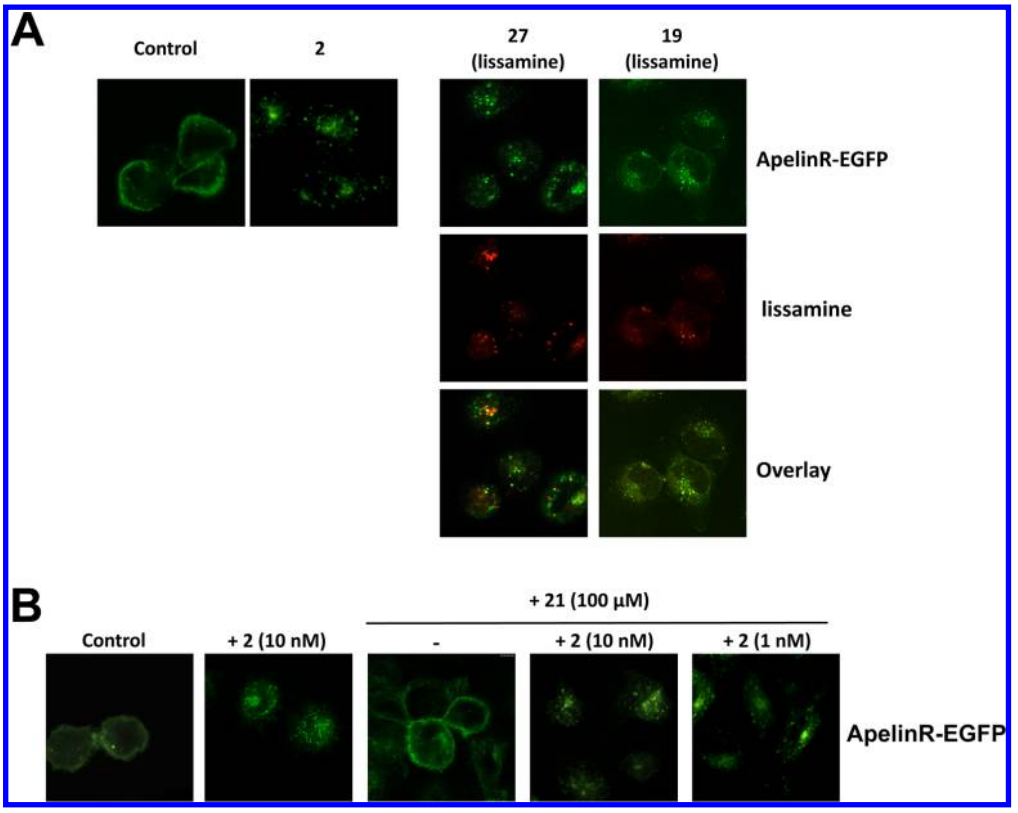

Figure 3. Effects of **2**, **27**, **19**, and **21** on rat ApelinR-EGFP internalization in CHO cells. (A) CHO cells stably expressing the rat ApelinR-EGFP were treated with **2** (100 nM), **27** (100 μM), or **19** (100 μM) for 20 min at 37 °C. Cells were fixed, and receptor internalization was analyzed by measuring EGFP fluorescence by confocal microscopy. (B) CHO cells stably expressing the rat ApelinR-EGFP were treated with either **2** (10 nM, 1 nM) or **21** (100 μM) or both for 20 min at 37 °C. Cells were fixed, and receptor internalization was analyzed by confocal microscopy.

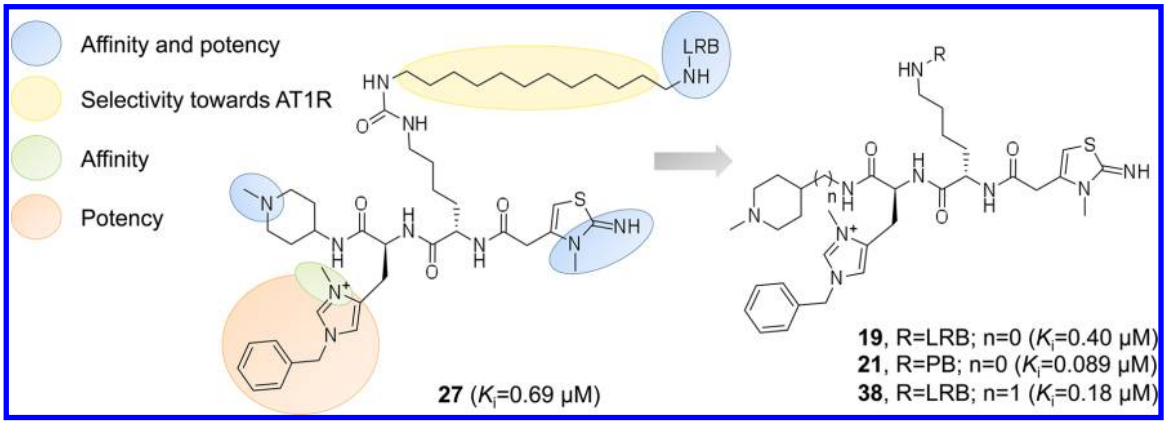

Figure 4. Summary of the structure–activity relationships around **27**: important structural determinants for both the affinity and the potency of the ligand to trigger ApelinR internalization.

family; (2) their effects on forskolin-induced cAMP production; and (3) their stability in mouse plasma.

Binding Selectivity and Effects on Forskolin-Induced cAMP Production. The selectivity of **27**, **19**, and **21** toward AT1R was evaluated by a radioligand binding assay. Whereas **27** displayed only a low 3-fold binding selectivity for both receptors, **19** exhibited a >2500-fold binding selectivity (AT1R/ApelinR). These data suggest that the shorter the spacer, the more selective is the compound. This was confirmed with **21** that displayed a 675-fold binding selectivity toward the ApelinR as compared to that of the AT1R. To investigate further their pharmacological profile, the effect of the three ligands on forskolin-induced cAMP production was evaluated. Incubation of CHO cells stably expressing the rat ApelinR in the presence of 5 μM forskolin with increasing concentrations of **2**, **27**, **19**, and **21** (10 nM to 100 μM) resulted in a concentration-dependent inhibition of forskolin-induced cAMP production (Figure 5) with IC_{50} values of 1.4×10^{-3}, 4.3, 3.0, and 1.7 μM, respectively (Table 5). The maximal inhibitory effects of these compounds on forskolin-induced cAMP production were 85 ± 13%, 100 ± 7%, 77 ± 15%, and 69 ± 14% for **2**, **27**, **19**, and **21**, respectively. Since **21** displaces the radioligand [^{125}I]-**3** in a competitive manner and since it inhibits cAMP production as apelin does, this suggests that **21** likely binds to the ApelinR at the same binding site as the endogenous peptides. The molecular mechanism of the biased

dx.doi.org/10.1021/jm401789v | J. Med. Chem. 2014, 57, 2908–2919

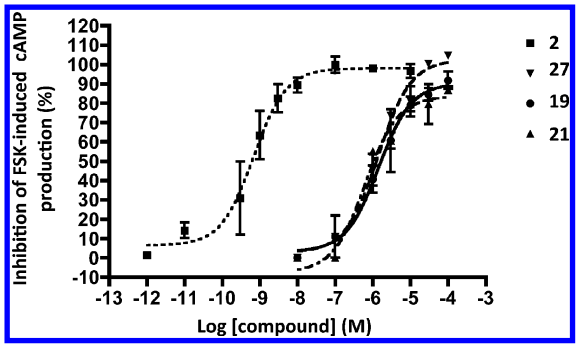

Figure 5. Effects of **2**, **27**, **19**, and **21** on forskolin-induced cAMP production in CHO cells stably expressing the rat ApelinR-EGFP. cAMP production was induced by treatment of cells with 5 μM forskolin. The effects of various concentrations of **2**, **27**, **19**, and **21** on forskolin-induced cAMP production were evaluated by HTRF (Cisbio). Sigmoidal dose–response curves are representative of three independent experiments performed in duplicate.

agonism is probably related to subtle differences in the interaction network at the orthosteric binding cavity. Altogether, these data suggest that **27** and **19** are full agonists with regard to cAMP production and ApelinR internalization, whereas **21** is a biased agonist toward cAMP production. Biased agonists trigger conformational changes of the signaling effectors such as G-protein and β-arrestin, different from those induced by unbiased agonists.[40,41] The development of such compounds could be therapeutically useful since biased agonists, by stabilizing the receptor in a defined conformation, could induce a specific apelin biological action.

Plasma Stability of Compounds 19, 21, and 27 in Mouse Plasma. The nonpeptidic character of **19**, **21**, and **27** prompted us to evaluate their stability in mouse plasma at 37 °C. Whereas the half-life stability of **2** is around 4.6 min, the three ApelinR ligands **27**, **19**, and **21** exhibit a much higher stability in mouse plasma ($T_{1/2}$ > 10 h), which opens the way to the *in vivo* evaluation of these compounds.

CONCLUSIONS

A new convenient synthetic route was developed to allow the study of the structure–activity relationships of the first described nonpeptidic ApelinR agonist **1**. This approach enabled the access to **27**, the major component of **1**. The structural determinants of its activity have been characterized leading to the discovery of **19** and **21**, two novel ligands of the ApelinR displaying lower molecular weights and higher affinities than **27**. In addition, **19** and **21** show an increased selectivity toward the AT1R, as compared to **27**. Interestingly, **19** is a full agonist with regard to cAMP production and ApelinR internalization, whereas **21** behaves as a biased agonist toward cAMP production. Finally, **19** and **21** display a much greater stability in mouse plasma than the endogenous apelin peptide **2** and represent therefore suitable pharmacological tools for *in vivo* studies. Considering their fluorescent properties, we anticipate that these probes could not only constitute convenient tools for *in vivo* labeling of the ApelinR but also improve our knowledge on its physiopathologic roles.

EXPERIMENTAL SECTION

General Methods. Reagents were obtained from commercial sources and used without any further purification. DFPE-PS resin (100–200 mesh, 0.92 mmol/g) was purchased from Novabiochem. Acid Red 52 sodium salt (Lissamine Rhodamine B sodium sulfonate) was obtained from TCI Europe (Zwijndrecht, Belgium). Patent Blue VF [129-17-9] was obtained from ACROS with a 50% dye content. Its conversion into activated sulfonyl chloride (PB-Cl) was performed following the experimental conditions previously reported.[42] Solid-phase reactions conducted at room temperature were performed in polypropylene tubes equipped with polyethylene frits and polypropylene caps using an orbital shaking device. Solid-phase reactions at higher temperatures were conducted in sealed glassware tubes using a Chemflex rotating oven from Robbins Scientific as the shaking device. Thin-layer chromatography was performed on silica gel 60F_{254} plates. Merck silica gel (Kieselgel 60; 230–400 mesh) was used for chromatography columns. Flash chromatography was performed on silica gel (40 μm, Grace) or RP18 (25–40 μm, Merck) prepacked columns on a SpotII ultimate from Armen or a PLC 2020 from Gilson. ^{1}H NMR spectra were recorded at 300 MHz or 400 MHz on a Bruker Advance spectrometer. Chemical shifts are reported in parts per million (ppm), and coupling constants (J) are reported in hertz (Hz). Analytical reverse-phase high performance liquid chromatography (RP-HPLC) separations were performed on C18 Ascentis Express (2.7 μm, 4.6 mm × 75 mm) using a linear gradient (5% to 100% of solvent B in solvent A in 7.5 min, flow rate of 1.6 mL·min^{-1}, detection at 220 nm; solvent A, water/0.1% TFA; solvent B, acetonitrile/0.1% TFA). Semipreparative reverse phase high performance liquid chromatography (RP-HPLC) separations were performed on a Waters XBridge RP-C_{18} column (5 μm, 19 × 100 mm) using a linear gradient (solvent B in solvent A; solvent A, water/0.1% TFA; solvent B, acetonitrile/0.1% TFA; flow rate of 20 mL·min^{-1}; detection at 220 nm). Purified final compounds eluted as single and symmetrical peaks (thereby confirming a purity of ≥95%) at the retention times (t_R) given below. High resolution mass spectra (HRMS) were acquired on a Bruker MicroTof mass spectrometer, using electrospray ionization (ESI) and a time-of-flight analyzer (TOF).

*Methyl (2-Imino-3-methyl-2,3-dihydrothiazol-4-yl)acetate hydroiodide (**5**).* Methyl iodide (38 mL, 0.610 mol) was added to a solution of commercially available compound **4** (10.50 g, 0.061 mol) in dry THF (110 mL), and the mixture was stirred at room temperature for 72 h. The mixture was filtered, and the precipitate was washed several times with cold THF and dried *in vacuo* to give the title compound (17.94 g, 93%) as a white solid. t_R = 0.49 min; mp 153–155 °C; ^{1}H

Table 5. Summary of Pharmacological Properties of 2, 27, 19, and 21

	binding affinity[a] (K_i, μM)[a]		binding selectivity		
cpd	ApelinR	AT1R	AT1R/ApelinR	inhibition of cAMP production (IC_{50}, μM)[b]	plasma half-life[c] ($T_{1/2}$)
2	0.04 ± 0.002 × 10^{-3}	>100	>10^5	1.4 ± 0.67 × 10^{-3}	4.6 min
27	0.69 ± 0.12	2.23 ± 0.7	3	4.3 ± 1.9	>10 h
19	0.40 ± 0.08	>1000	2630	3.0 ± 0.7	>10 h
21	0.089 ± 0.014	98 ± 30	675	1.7 ± 0.8	>10 h

[a]The inhibition constants (K_i) of the compounds for the ApelinR or AT1R were determined on CHO cell membranes expressing either the human ApelinR or the human AT1R by competition binding assays using as radioligand either [^{125}I]-**3** or [^{125}I]-angiotensin II. [b]cAMP was quantified using the cAMP dynamic 2 assay kit (Cisbio Bioassays, see Experimental Section). Data represent the means ± SE of 3 to 4 independent experiments performed in duplicate. [c]Stability was evaluated in mouse plasma at 37 °C (see Experimental Section).

dx.doi.org/10.1021/jm401789v | J. Med. Chem. 2014, 57, 2908–2919

NMR (DMSO-d_6, 400 MHz) δ 9.39 (br s, 2H), 6.94 (s, 1H), 3.97 (s, 2H), 3.67 (s, 3H), 3.44 (s, 3H); ^{13}C NMR (DMSO-d_6, 100 MHz) δ 168.8, 168.4, 134.4, 105.8, 52.4, 33.1, 32.5.

*(2-Imino-3-methyl-2,3-dihydrothiazol-4-yl)acetic Acid Hydrochloride (**6**).* 1 N HCl (6.6 mL, 6.6 mmol) was slowly added to a solution of **5** (82.0 mg, 0.26 mmol) in dioxane/water, 2/1 (4.1 mL), and the mixture was stirred at 40 °C for 19 h. It was then concentrated *in vacuo*, and EtOAc was added to the crude. A precipitate formed, which was collected by filtration, washed with cold EtOAc, and dried under vacuum to give the title compound (47.6 mg, 88%) as a white-gray solid. mp 172−174 °C. ^{1}H NMR (400 MHz, DMSO-d_6) δ 9.53 (br s, 1H), 6.90 (s, 1H), 3.84 (s, 2H), 3.46 (s, 3H); ^{13}C NMR (100 MHz, DMSO-d_6) δ 169.9, 168.4, 135.2, 105.2, 33.2, 33.0. HRMS (ESI) calcd for $C_6H_9N_2O_2S$ ($[M + H]^+$) 173.0384; found, 173.0377.

*Methyl 2-(tert-Butoxycarbonylimino-3-methyl-2,3-dihydrothiazol-4-yl)acetate (**7**).* Compound **5** (4.0 g, 12.7 mmol) was added portionwise to a solution of di-*tert*-butyl dicarbonate (13.9 g, 63.7 mmol), DMAP (476 mg, 3.9 mmol), and triethylamine (4.6 mL, 32.9 mmol) in dry THF (80 mL), under an argon atmosphere. The mixture was heated to reflux for 4 h then cooled to room temperature and filtered. The filtrate was concentrated and the crude product purified by column chromatography (5% methanol in CH_2Cl_2), affording the title compound (3.26 g, 61%) as a white solid. t_R = 3.08 min; mp 126−128 °C; ^{1}H NMR ($CDCl_3$, 400 MHz) δ 6.37 (s, 1H), 3.68 (s, 3H), 3.59 (s, 2H), 3.53 (s, 3H), 1.49 (s, 9H); ^{13}C NMR ($CDCl_3$, 100 MHz) δ 170.7, 168.7, 162.3, 130.8, 106.4, 79.9, 52.8, 33.9, 33.2, 28.5.

*2-(tert-Butoxycarbonylimino-3-methyl-2,3-dihydrothiazol-4-yl)-acetic Acid (**8**).* Lithium hydroxide (1.44 g, 60.1 mmol) was added to a solution of 7 (2.50 g, 8.7 mmol) in dioxane/water, 2/1 (60 mL), and the mixture was stirred at 40 °C for 1 h, then cooled to room temperature. The pH of the solution was adjusted to pH 4 by the addition of citric acid, and the aqueous layer was extracted several times with CH_2Cl_2. The combined organic extracts were washed with brine, dried over sodium sulfate, and concentrated. The residue was dissolved in the minimum amount of Et_2O, and *n*-heptane was added. The mixture was sonicated and filtered, and the precipitate was washed with cold *n*-heptane and dried *in vacuo* to give the title compound (1.47 g, 61%) as a white solid. t_R = 2.96 min; mp 107−109 °C; ^{1}H NMR ($CDCl_3$, 400 MHz) δ 9.05 (sl, 1H), 6.45 (s, 1H), 3.61 (s, 2H), 3.55 (s, 3H), 1.48 (s, 9H); ^{13}C NMR ($CDCl_3$, 100 MHz) δ 17.1.6, 170.1, 161.0, 132.2, 107.2, 80.5, 34.3, 33.7, 28.4; HRMS (ESI) calcd for $C_{11}H_{16}N_2O_4S$ ($[M]^+$) 272.0830; found, 272.0818.

*Synthesis of Resin **9** from DFPE Resin.* A mixture of DFPE resin (loading: 0.92 mmol/g), 4-amino-1-Boc-piperidine (5 equiv), and sodium cyanoborohydride (5 equiv) in DMF/MeOH/AcOH, 80/19/1 (10 mL/g of resin), was shaken at 60 °C overnight. The solution was drained, and the resin was washed in sequence with DMF, CH_2Cl_2, and MeOH, then dried under vacuum for 24 h. The resin was swollen in CH_2Cl_2, and the excess solvent was removed by filtration. In a separate vial, DIEA (12.5 equiv) was added to a solution of Fmoc-His(1-Bzl)-OH (5 equiv) and HATU (4.95 equiv) in DMF/CH_2Cl_2, 4/1 (15 mL/g of resin). After 1 min, the resulting solution was added to the resin, and the mixture was shaken at room temperature overnight. The solution was drained, and the resin was washed with DMF, CH_2Cl_2, MeOH, and dried under vacuum.

*Synthesis of Resin **10**.* To resin **9**, swollen in DMF (10 mL/g of resin), was added methyl iodide (40 equiv), and the mixture was shaken at 40 °C overnight. The solution was drained, and the resin was washed in sequence with DMF, CH_2Cl_2, and MeOH. The resin was then swollen in CH_2Cl_2, the excess solvent was removed by filtration, and the resin dried under vacuum for no less than 24 h. To ensure completion of the reaction, a small sample of resin was treated with TFA/H_2O/triisopropylsilane (TIS), 95/2.5/2.5, and the solution was collected, evaporated *in vacuo*, and analyzed by LC-MS.

*Synthesis of Resin **11**.* Resin **10** was swollen in dry CH_2Cl_2, and the excess solvent removed by filtration. In a separate vial, freshly prepared solutions of TMSOTf (0.4 M in dry CH_2Cl_2, 10 mL/g of resin) and 2,6-lutidine (0.8 M in dry CH_2Cl_2, 10 mL/g of resin) were combined and added to the resin. The mixture was shaken at room temperature for 30 min. The solution was drained, and the reaction was repeated for another 30 min. The solution was drained, and the resin was washed first with dry CH_2Cl_2 and then with dry THF. To the resin, swollen in dry THF/$HC(OCH_3)_3$, 1/1 (20 mL/g of resin), formaldehyde (37 wt % in water, 40 equiv) was added, and the mixture was shaken at room temperature for 5 h. The solution was drained, and the resin was washed with dry 1,2-dichloroethane (1,2-DCE). A suspension of sodium triacetoxyborohydride (20 equiv) in dry 1,2-DCE (20 mL/g of resin) was added, and the mixture was shaken at room temperature overnight. The solution was drained, and the resin washed with DMF, CH_2Cl_2, and MeOH. To ensure completion of the reaction, a small sample of resin was treated with TFA/H_2O/TIS, 95/2.5/2.5, the solution was collected, evaporated *in vacuo*, and analyzed by LC-MS.

*Synthesis of Resin **12**.* Resin **12** was prepared as resin **11**, except that formaldehyde was replaced by benzaldehyde (20 equiv).

General Experimental Procedure for the Synthesis of Resins 13 and 14 from Resins 11 and 12, Respectively. The resin was swollen in DMF, and the excess solvent was removed by filtration. A solution of piperidine in DMF (20% v/v−15 mL/g of resin) was added, and the mixture was shaken at room temperature for 10 min. The solution was drained, and the operation was repeated for 15 min. The solution was drained and the resin was washed with DMF, CH_2Cl_2, and MeOH. The resin was again swollen in DMF, and the excess solvent was removed by filtration. A solution of Fmoc-Lys(ivDde)-OH (5 equiv), PyBOP, (5 equiv), and HOBt (5 equiv) in DMF (15 mL/g of resin) was added followed by *N*,*N*-diisopropylethylamine (DIEA) (12.5 equiv), and the mixture was shaken at room temperature for 2 h. The solution was drained, and the resin was washed with DMF, CH_2Cl_2, and MeOH. The resin was again treated with piperidine in DMF as described above. A solution of **8** (4 equiv), PyBOP, (4 equiv), and HOBt (4 equiv) in CH_2Cl_2/DMF, 4/1 (15 mL/g of resin), was added followed by DIEA (10 equiv), and the mixture was shaken at room temperature overnight. The solution was drained, and the resin was washed with DMF, CH_2Cl_2, and MeOH. The resin was swollen in DMF, and the excess solvent was removed by filtration. A solution of hydrazine hydrate in DMF (5% v/v−15 mL/g of resin) was then added, and the mixture was shaken at room temperature for 5 min. The solution was drained, and the hydrazine treatment was repeated twice. The resin was washed with DMF, CH_2Cl_2, and MeOH.

General Experimental Procedure for the Synthesis of Resins 15 and 17 from Resin 13 and of Resin 16 from Resin 14. The resin was swollen in dry CH_2Cl_2, and the excess solvent was removed by filtration. A solution of LRB-Cl or PB-Cl (2 equiv) in dry CH_2Cl_2 (25 mL/g of resin) was added followed by DIEA (3 equiv). The mixture was shaken at room temperature for 5 h, and the solution was drained. The resin was washed successively with 10% DIEA in DMF, THF/H_2O, 3/2, DMF, CH_2Cl_2, and MeOH, and those washings were repeated at least 5 times. The resin was then washed with Et_2O and dried under vacuum.

*Synthesis of Resin **18**.* Acetic anhydride (10 equiv) and DIEA (10 equiv) were added to resin **13** and swollen in dry CH_2Cl_2 (10 mL/g of resin), and the mixture was shaken at room temperature for 10 min. The solution was drained, and the treatment was repeated once. The solution was drained, the resin washed with DMF, CH_2Cl_2, and MeOH, and dried under vacuum.

General Experimental Procedure for the Synthesis of Resins 23 and 24. Resin **13** was swollen in dry CH_2Cl_2 and the excess solvent was removed by filtration. A solution of 4-nitrophenyl chloroformate (5 equiv) in dry THF/CH_2Cl_2, 1/1 (40 mL/g of resin), was added followed by DIEA (5 equiv). The mixture was shaken at room temperature for 45 min, and the solution was drained. The procedure was repeated once. The resin was washed with CH_2Cl_2 and Et_2O before being transferred into a microwave tube. A suspension of diamine $H_2NCH_2(CH_2)_nCH_2NH_2$ (n = 4 or 10, 20 equiv) in 1,2-DCE (40 mL/g of resin) was added, the tube was sealed, and the mixture was shaken at 30 °C overnight. The resin was filtered and washed with DMF, CH_2Cl_2, and MeOH.

Synthesis of Resins ***25*** *and* ***26*** *from Resins* ***23*** *and* ***24****, Respectively*. Resins **23** and **24** were labeled with LRB-Cl as described previously for resins **15** and **16**.

General Experimental Procedure for the Cleavage of the Products from the Resin. The dried resin was treated with TFA/H_2O/TIS, 95/2.5/2.5 (25 mL/g of resin), and the mixture was shaken at room temperature for 3 h. The solution was collected and the beads washed with TFA. The solution was evaporated *in vacuo* and the crude product purified by semipreparative RP-HPLC. Lyophilization afforded the expected product.

Compound ***19***. Prepared on a 690 μmol scale. Pink solid (44.0 mg, 4%). t_R = 3.71 min. (>95% purity [220 nm]); HRMS (ESI) calcd for $C_{59}H_{76}N_{11}O_9S_3$ ($[M]^+$) 1178.4989; found, 1178.4967.

Compound ***20***. Prepared on a 50 μmol scale. Pink solid (23.9 mg, 30%). t_R = 3.88 min. (>97% purity [220 nm]); HRMS (ESI) calcd for $C_{65}H_{81}N_{11}O_9S_3$ ($[M + H]^{2+}$) 627.7690; found, 627.7702.

Compound ***21***. Prepared on a 115 μmol scale. Blue solid (17.8 mg, 10%). t_R = 3.47 min. (>98% purity [220 nm]); HRMS (ESI) calcd for $C_{59}H_{78}N_{11}O_8S_3$ ($[M]^+$) 1164.5197; found, 1164.5193.

Compound ***22***. Prepared on a 55 μmol scale. White solid (8.2 mg, 15%). t_R = 2.00/2.06 min. (>98% purity [220 nm]); MS (ESI) *m*/*z* 680.2 ($[M]^+$), 340.8 ($[M + H]^{2+}$).

Compound ***27***. Prepared on a 560 μmol scale. Pink solid (8.8 mg, 2%). t_R = 4.82 min. (>95% purity [220 nm]); HRMS (ESI) calcd for $C_{72}H_{102}N_{13}O_{10}S_3$ ($[M + H]^{2+}$) 702.3517; found, 702.8568.

Compound ***28***. Prepared on a 110 μmol scale. Pink solid (14.6 mg, 8%). HRMS (ESI) calcd for $C_{66}H_{92}N_{13}O_{10}S_3$ ($[M + H]^{2+}$) 660.8087; found, 660.8062.

Stability in Mouse Plasma. Stability of compounds **2**, **27**, **19**, and **21** was determined in mouse plasma at 37 °C. For each compound, the stock solution (100 μM in water) was diluted in plasma to a final incubation concentration of 5 μM. The incubation at 37 °C was stopped at t_0 and 24 h by adding one volume of ice cold acetonitrile containing 0.1% trifluoroacetic acid. The sample was vortexed for 1 min and then centrifuged at 4 °C before LC-MS injection of the supernatant. Analyses were performed on a Kinetex RP-C_{18} column (2.6 μm, 100 Å, 50 × 4.6 mm) using a linear gradient (solvent B in solvent A, solvent A, water/0.05% TFA; solvent B, acetonitrile; flow rate of 2 mL·min^{-1}; detection at 358 nm). The percentage of the remaining test compound relative to t_0 was measured by monitoring the peak area of the chromatogram.

Radioligand Binding Experiments. Membrane preparation from CHO cells stably expressing the human ApelinR or the human angiotensin II receptor type 1 were purchased from Perkin-Elmer (Perkin-Elmer, Wellesley, MA, USA). Membrane preparations (0.5 μg of total mass of membranes/assay) were incubated for 1 h at 20 °C with 0.2 nM [^{125}I]-**3** (Perkin-Elmer) or with 0.1 nM [^{125}I]-angiotensin II (Perkin-Elmer) in binding buffer (50 mM Hepes, 5 mM $MgCl_2$ at pH 7.5, BSA 1%) alone or in the presence of the different compounds to be tested at various concentrations. The reaction was stopped by adding 4 mL of cold binding buffer and filtered on Whatman GF/C filters. After washing, radioactivity was counted with a Wizard 1470 Wallac gamma counter (Perkin-Elmer, Turku, Finland).

cAMP Assay. cAMP was quantified using the cAMP dynamic 2 assay kit (Cisbio Bioassays, Codolet, France). CHO cells stably expressing ApelinR-EGFP (1×10^6 cells/well) were seeded in 96 wells plates previously coated with polylysine (WI; 0.01%) (Sigma-Aldrich, St Quentin, France) and incubated for 24 h before treatment. After the following day, cells were stimulated with 100 μL of stimulation buffer (HBSS, 5 mM Hepes, 0.1% BSA stabilizer, and 1 mM IBMX, pH 7.4) containing 5 μM forskolin (FSK) and increasing concentrations of the test compound (10 nM to 100 μM) for 30 min at 37 °C. Cells were then washed 3 times with 100 μL of stimulation buffer. Finally, for each well we added 50 μL of stimulation buffer, 25 μL of anti-cAMP antibody cryptate, and 25 μL of cAMP D2. After 1 h of incubation at 20 °C, fluorescence was measured using an EnVision Xcite Multilabel Reader (Perkin-Elmer, Wellesley, MA, USA).

ApelinR Internalization Studies. CHO cells stably expressing the rat ApelinR-EGFP were seeded at 40% confluency on glass coverslips coated with polylysine (weight/volume 0.01%) (Sigma-Aldrich, St. Quentin, France) and incubated for 30 min at 37 °C. Then cells were incubated for 90 min at 37 °C with 90 μM of cycloheximide (Sigma-Aldrich, St. Quentin, France). Internalization was performed by incubating the cells for 20 min at 37 °C with 1 nM, 10 nM, and 100 nM of **2** or 100 mM of **19**, **21**, and **27** as described previously.[13] Cells were then mounted in Aquapolymount (Polysciences, Warrington, PA, USA) for confocal microscopic analysis.

Confocal Microscopy. The cells were examined with a Leica TCS SP5MP (Leica Microsystems, Heidelberg, Germany) equipped with an argon ion laser adjusted to 488 nm for GFP and a helium neon laser adjusted to 568 nm for LRB. Sections were scanned, and double-labeled images were obtained with two photomultipliers and appropriate filter settings for the separate detection of fluorescence from GFP and LRB. Optical sections (1024 × 1024) of individual cells were taken at the equatorial level (level of the nucleus), using a 63xNA oil-immersion objective.

■ ASSOCIATED CONTENT

Ⓢ Supporting Information

General procedure for the preparation of compounds **29**−**40**; pK_a determination for **4** and **5**; RP-HPLC, CZE, and MS/MS analysis of **1** (Figures S1, S2, and S3, respectively), and confocal microscopy monitoring of the ability of **20**, **37**, **38**, and **40** to trigger rat ApelinR internalization (Figure S4). This material is available free of charge via the Internet at http://pubs.acs.org.

■ AUTHOR INFORMATION

Corresponding Authors

*(C.L.-C.) Phone: +33 1 44 27 16 63. E-mail: c.llorens-cortes@college-de-france.fr.

*(D.B.) Phone: +33 368 85 42 36. E-mail: dominique.bonnet@unistra.fr

Author Contributions

§J.-F.M. and X.I. contributed equally to this work.

Author Contributions

‖C.L.-C. and D.B. are co-last authors.

Notes

The authors declare no competing financial interest.

■ ACKNOWLEDGMENTS

J.-F.M. was supported by the Agence Nationale pour la Recherche (ANR Physique et Chimie du Vivant 2008), the Centre National de la Recherche Scientifique, the Université de Strasbourg, and the Institut National de la Santé et de la Recherche Médicale. We are grateful to Patrick Wehrung for ES-MS analyses, to Dr. Agnès Hagège for CZE analysis, and to Dr. Patrick Gizzi for stability studies.

■ ABBREVIATIONS USED

AT1R, angiotensin II receptor type 1; ApelinR, apelin receptor; AVP, arginine-vasopressine; DFPE, 2-(3,5-dimethoxy-4-formylphenoxy)ethyl; EGFP, enhanced green fluorescent protein; FRET, fluorescence resonance energy transfer; GPCRs, G protein-coupled receptors; HBTU, *N*-[(1*H*benzotriazol-1-yl)(dimethylamino)methylene]-*N*-methylmethanaminium hexafluorophosphate *N*-oxide; HOBt, *N*-hydroxybenzotriazole; HRMS, high resolution mass spectrometry; LRB, Lissamine Rhodamine B; PB-Cl, Patent Blue sulfonyl chloride; MS, mass spectrometry; PyBOP, (benzotriazol-1-yl-oxy)-trispyrrolidinophosphonium hexafluorophosphate; REM, regenerative Michael acceptor; TIS, triisopropylsilane; TMSOTf, trimethylsilyl trifluoromethanesulfonate

REFERENCES

(1) Tatemoto, K.; Hosoya, M.; Habata, Y.; Fujii, R.; Kakegawa, T.; Zou, M. X.; Kawamata, Y.; Fukusumi, S.; Hinuma, S.; Kitada, C.; Kurokawa, T.; Onda, H.; Fujino, M. Isolation and characterization of a novel endogenous peptide ligand for the human APJ receptor. *Biochem. Biophys. Res. Commun.* **1998**, *251*, 471−476.

(2) O'Dowd, B. F.; Heiber, M.; Chan, A.; Heng, H. H.; Tsui, L. C.; Kennedy, J. L.; Shi, X.; Petronis, A.; George, S. R.; Nguyen, T. A human gene that shows identity with the gene encoding the angiotensin receptor is located on chromosome 11. *Gene* **1993**, *136*, 355−360.

(3) Devic, E.; Rizzoti, K.; Bodin, S.; Knibiehler, B.; Audigier, Y. Amino acid sequence and embryonic expression of msr/apj, the mouse homolog of Xenopus X-msr and human APJ. *Mech. Dev.* **1999**, *84*, 199−203.

(4) De Mota, N.; Lenkei, Z.; Llorens-Cortes, C. Cloning, pharmacological characterization and brain distribution of the rat apelin receptor. *Neuroendocrinology* **2000**, *72*, 400−407.

(5) Habata, Y.; Fujii, R.; Hosoya, M.; Fukusumi, S.; Kawamata, Y.; Hinuma, S.; Kitada, C.; Nishizawa, N.; Murosaki, S.; Kurokawa, T.; Onda, H.; Tatemoto, K.; Fujino, M. Apelin, the natural ligand of the orphan receptor APJ, is abundantly secreted in the colostrum. *Biochim. Biophys. Acta* **1999**, *1452*, 25−35.

(6) Lee, D. K.; Cheng, R.; Nguyen, T.; Fan, T.; Kariyawasam, A. P.; Liu, Y.; Osmond, D. H.; George, S. R.; O'Dowd, B. F. Characterization of apelin, the ligand for the APJ receptor. *J. Neurochem.* **2000**, *74*, 34−41.

(7) Azizi, M.; Iturrioz, X.; Blanchard, A.; Peyrard, S.; De Mota, N.; Chartrel, N.; Vaudry, H.; Corvol, P.; Llorens-Cortes, C. Reciprocal regulation of plasma apelin and vasopressin by osmotic stimuli. *J. Am. Soc. Nephrol.* **2008**, *19*, 1015−1024.

(8) De Mota, N.; Reaux-Le Goazigo, A.; El Messari, S.; Chartrel, N.; Roesch, D.; Dujardin, C.; Kordon, C.; Vaudry, H.; Moos, F.; Llorens-Cortes, C. Apelin, a potent diuretic neuropeptide counteracting vasopressin actions through inhibition of vasopressin neuron activity and vasopressin release. *Proc. Natl. Acad. Sci. U.S.A.* **2004**, *101*, 10464−10469.

(9) Iturrioz, X.; Gerbier, R.; Leroux, V.; Alvear-Perez, R.; Maigret, B.; Llorens-Cortes, C. By interacting with the C-terminal Phe of apelin, Phe255 and Trp259 in helix VI of the apelin receptor are critical for internalization. *J. Biol. Chem.* **2010**, *285*, 32627−32637.

(10) Medhurst, A. D.; Jennings, C. A.; Robbins, M. J.; Davis, R. P.; Ellis, C.; Winborn, K. Y.; Lawrie, K. W.; Hervieu, G.; Riley, G.; Bolaky, J. E.; Herrity, N. C.; Murdock, P.; Darker, J. G. Pharmacological and immunohistochemical characterization of the APJ receptor and its endogenous ligand apelin. *J. Neurochem.* **2003**, *84*, 1162−1172.

(11) Zhou, N.; Fan, X.; Mukhtar, M.; Fang, J.; Patel, C. A.; DuBois, G. C.; Pomerantz, R. J. Cell-cell fusion and internalization of the CNS-based, HIV-1 co-receptor, APJ. *Virology* **2003**, *307*, 22−36.

(12) Iturrioz, X.; Alvear-Perez, R.; De Mota, N.; Franchet, C.; Guillier, F.; Leroux, V.; Dabire, H.; Le Jouan, M.; Chabane, H.; Gerbier, R.; Bonnet, D.; Berdeaux, A.; Maigret, B.; Galzi, J. L.; Hibert, M.; Llorens-Cortes, C. Identification and pharmacological properties of E339−3D6, the first nonpeptidic apelin receptor agonist. *FASEB J.* **2010**, *24*, 1506−1517.

(13) El Messari, S.; Iturrioz, X.; Fassot, C.; De Mota, N.; Roesch, D.; Llorens-Cortes, C. Functional dissociation of apelin receptor signaling and endocytosis: implications for the effects of apelin on arterial blood pressure. *J. Neurochem.* **2004**, *90*, 1290−1301.

(14) Evans, N. A.; Groarke, D. A.; Warrack, J.; Greenwood, C. J.; Dodgson, K.; Milligan, G.; Wilson, S. Visualizing differences in ligand-induced beta-arrestin-GFP interactions and trafficking between three recently characterized G protein-coupled receptors. *J. Neurochem.* **2001**, *77*, 476−485.

(15) Reaux, A.; De Mota, N.; Skultetyova, I.; Lenkei, Z.; El Messari, S.; Gallatz, K.; Corvol, P.; Palkovits, M.; Llorens-Cortes, C. Physiological role of a novel neuropeptide, apelin, and its receptor in the rat brain. *J. Neurochem.* **2001**, *77*, 1085−1096.

(16) Brailoiu, G. C.; Dun, S. L.; Yang, J.; Ohsawa, M.; Chang, J. K.; Dun, N. J. Apelin-immunoreactivity in the rat hypothalamus and pituitary. *Neurosci. Lett.* **2002**, *327*, 193−1997.

(17) O'Carroll, A. M.; Selby, T. L.; Palkovits, M.; Lolait, S. J. Distribution of mRNA encoding B78/apj, the rat homologue of the human APJ receptor, and its endogenous ligand apelin in brain and peripheral tissues. *Biochim. Biophys. Acta* **2000**, *1492*, 72−80.

(18) Reaux, A.; Gallatz, K.; Palkovits, M.; Llorens-Cortes, C. Distribution of apelin-synthesizing neurons in the adult rat brain. *Neuroscience (Oxford, U.K.)* **2002**, *113*, 653−662.

(19) O'Carroll, A. M.; Don, A. L.; Lolait, S. J. APJ receptor mRNA expression in the rat hypothalamic paraventricular nucleus: regulation by stress and glucocorticoids. *J. Neuroendocrinol.* **2003**, *15*, 1095−1101.

(20) Reaux-Le Goazigo, A.; Morinville, A.; Burlet, A.; Llorens-Cortes, C.; Beaudet, A. Dehydration-induced cross-regulation of apelin and vasopressin immunoreactivity levels in magnocellular hypothalamic neurons. *Endocrinology* **2004**, *145*, 4392−4400.

(21) Japp, A. G.; Cruden, N. L.; Amer, D. A.; Li, V. K.; Goudie, E. B.; Johnston, N. R.; Sharma, S.; Neilson, I.; Webb, D. J.; Megson, I. L.; Flapan, A. D.; Newby, D. E. Vascular effects of apelin in vivo in man. *J. Am. Coll. Cardiol.* **2008**, *52*, 908−913.

(22) Ashley, E. A.; Powers, J.; Chen, M.; Kundu, R.; Finsterbach, T.; Caffarelli, A.; Deng, A.; Eichhorn, J.; Mahajan, R.; Agrawal, R.; Greve, J.; Robbins, R.; Patterson, A. J.; Bernstein, D.; Quertermous, T. The endogenous peptide apelin potently improves cardiac contractility and reduces cardiac loading in vivo. *Cardiovasc. Res.* **2005**, *65*, 73−82.

(23) Berry, M. F.; Pirolli, T. J.; Jayasankar, V.; Burdick, J.; Morine, K. J.; Gardner, T. J.; Woo, Y. J. Apelin has in vivo inotropic effects on normal and failing hearts. *Circulation* **2004**, *110*, 187−193.

(24) Szokodi, I.; Tavi, P.; Foldes, G.; Voutilainen-Myllyla, S.; Ilves, M.; Tokola, H.; Pikkarainen, S.; Piuhola, J.; Rysa, J.; Toth, M.; Ruskoaho, H. Apelin, the novel endogenous ligand of the orphan receptor APJ, regulates cardiac contractility. *Circ. Res.* **2002**, *91*, 434−440.

(25) Kuba, K.; Zhang, L.; Imai, Y.; Arab, S.; Chen, M.; Maekawa, Y.; Leschnik, M.; Leibbrandt, A.; Markovic, M.; Schwaighofer, J.; Beetz, N.; Musialek, R.; Neely, G. G.; Komnenovic, V.; Kolm, U.; Metzler, B.; Ricci, R.; Hara, H.; Meixner, A.; Nghiem, M.; Chen, X.; Dawood, F.; Wong, K. M.; Sarao, R.; Cukerman, E.; Kimura, A.; Hein, L.; Thalhammer, J.; Liu, P. P.; Penninger, J. M. Impaired heart contractility in Apelin gene-deficient mice associated with aging and pressure overload. *Circ. Res.* **2007**, *101*, 32−42.

(26) Tatemoto, K.; Takayama, K.; Zou, M. X.; Kumaki, I.; Zhang, W.; Kumano, K.; Fujimiya, M. The novel peptide apelin lowers blood pressure via a nitric oxide-dependent mechanism. *Regul. Pept.* **2001**, *99*, 87−92.

(27) Lee, D. K.; Saldivia, V. R.; Nguyen, T.; Cheng, R.; George, S. R.; O'Dowd, B. F. Modification of the terminal residue of apelin-13 antagonizes its hypotensive action. *Endocrinology* **2005**, *146*, 231−236.

(28) Boucher, J.; Masri, B.; Daviaud, D.; Gesta, S.; Guigne, C.; Mazzucotelli, A.; Castan-Laurell, I.; Tack, I.; Knibiehler, B.; Carpene, C.; Audigier, Y.; Saulnier-Blache, J. S.; Valet, P. Apelin, a newly identified adipokine up-regulated by insulin and obesity. *Endocrinology* **2005**, *146*, 1764−1771.

(29) Murza, A.; Parent, A.; Besserer-Offroy, E.; Tremblay, H.; Karadereye, F.; Beaudet, N.; Leduc, R.; Sarret, P.; Marsault, E. Elucidation of the structure-activity relationships of apelin: influence of unnatural amino acids on binding, signaling, and plasma stability. *Chem. Med. Chem.* **2012**, *7*, 318−325.

(30) Hamada, J.; Kimura, J.; Ishida, J.; Kohda, T.; Morishita, S.; Ichihara, S.; Fukamizu, A. Evaluation of novel cyclic analogues of apelin. *Int. J. Mol. Med.* **2008**, *22*, 547−552.

(31) Macaluso, N. J.; Pitkin, S. L.; Maguire, J. J.; Davenport, A. P.; Glen, R. C. Discovery of a competitive apelin receptor (APJ) antagonist. *Chem. Med. Chem.* **2011**, *6*, 1017−1023.

(32) Macaluso, N. J. M.; Glen, R. C. Exploring the 'RPRL' Motif of Apelin-13 through Molecular Simulation and Biological Evaluation of Cyclic Peptide Analogues. *Chem. Med. Chem.* **2010**, *5*, 1247−1253.

(33) Maloney, P. R.; Khan, P.; Hedrick, M.; Gosalia, P.; Milewski, M.; Li, L.; Roth, G. P.; Sergienko, E.; Suyama, E.; Sugarman, E.; Nguyen, K.; Mehta, A.; Vasile, S.; Su, Y.; Stonich, D.; Nguyen, H.; Zeng, F. Y.; Novo, A. M.; Vicchiarelli, M.; Diwan, J.; Chung, T. D.; Smith, L. H.; Pinkerton, A. B. Discovery of 4-oxo-6-((pyrimidin-2-ylthio)methyl)-4H-pyran-3-yl 4-nitrobenzoate (ML221) as a functional antagonist of the apelin (APJ) receptor. *Bioorg. Med. Chem. Lett.* **2012**, *22*, 6656−6660.

(34) Hibert, M.; Franchet, C. A., Galzi, J. L.; Pattus, F.; Guillier, F. Collections of Traceable Compounds and Uses Thereof. Patent WO 2006003329 A1, 2006.

(35) Toy, P. H.; Reger, T. S.; Janda, K. D. Soluble polymer bound cleavage reagents: A multipolymer strategy for the cleavage of tertiary amines from REM resin. *Org. Lett.* **2000**, *2*, 2205−2207.

(36) Bonnet, D.; Riche, S.; Loison, S.; Dagher, R.; Frantz, M. C.; Boudier, L.; Rahmeh, R.; Mouillac, B.; Haiech, J.; Hibert, M. Solid-phase organic tagging resins for labeling biomolecules by 1,3-dipolar cycloaddition: Application to the synthesis of a fluorescent non-peptidic vasopressin receptor ligand. *Chem.—Eur. J.* **2008**, *14*, 6247−6254.

(37) Zhang, A. J.; Russell, D. H.; Zhu, J. P.; Burgess, K. A method for removal of N-BOC protecting groups from substrates on TFA-sensitive resins. *Tetrahedron Lett.* **1998**, *39*, 7439−7442.

(38) Yang, H.; Vasudevan, S.; Oriakhi, C. O.; Shields, J.; Carter, R. G. Scalable synthesis of lissamine rhodamine B sulfonyl chloride and incorporation of xanthene derivatives onto polymer supports. *Synthesis* **2008**, *6*, 957−961.

(39) Papadopouloudaifotis, Z.; Costakis, E.; Tsatsas, G.; Varonos, D. Synthesis and pharmacological activity of some 2-imino-3-alkyl thiazoline derivatives. *Eur. J. Med. Chem.* **1979**, *14*, 253−256.

(40) Sauliere, A.; Bellot, M.; Paris, H.; Denis, C.; Finana, F.; Hansen, J. T.; Altie, M. F.; Seguelas, M. H.; Pathak, A.; Hansen, J. L.; Senard, J. M.; Gales, C. Deciphering biased-agonism complexity reveals a new active AT(1) receptor entity. *Nat. Chem. Biol.* **2012**, *8*, 622−630.

(41) Shukla, A. K.; Violin, J. D.; Whalen, E. J.; Gesty-Palmer, D.; Shenoy, S. K.; Lefkowitz, R. J. Distinct conformational changes in beta-arrestin report biased agonism at seven-transmembrane receptors. *Proc. Natl. Acad. Sci. U.S.A.* **2008**, *105*, 9988−9993.

(42) Bonnet, D.; Ilien, B.; Galzi, J. L.; Riche, S.; Antheaune, C.; Hibert, M. A rapid and versatile method to label receptor ligands using "click" chemistry: Validation with the muscarinic M1 antagonist pirenzepine. *Bioconjugate Chem.* **2006**, *17*, 1618−1623.